Mutations Synthetically Lethal With *tpm1Δ* Lie in Genes Involved in Morphogenesis

Tongtong Wang and Anthony Bretscher

Section of Biochemistry, Molecular and Cell Biology, Cornell University, Ithaca, New York 14853

Manuscript received April 23, 1997
Accepted for publication September 3, 1997

ABSTRACT

Yeast contains two genes, *TPM1* and *TPM2*, encoding tropomyosins, either of which can provide an essential function in the yeast cytoskeleton. To elucidate more clearly the function of the major tropomyosin, encoded by *TPM1*, we have isolated mutations that confer synthetic lethality with the null mutant of *TPM1*. Here we describe a phenotypic and genetic analysis of mutations in *TSL1/BEM2*, *TSL2*, *TSL3*, *TSL5*, and *TSL6* (tropomyosin synthetic lethal). All the mutants exhibit clear morphological and some actin cytoskeletal defects, but are not noticeably defective in secretion, endocytosis, or organelle segregation. The lethality conferred by *tsl tpm1Δ* mutations could be specifically suppressed by either *TPM1* or an additional copy of *TPM2*. This implies that the essential function compromised in the *tsl tpm1Δ* constructs is the same essential function for which Tpm1p or Tpm2p is necessary. Synthetic interactions and unlinked noncomplementation were observed between the *tsl* mutants, suggesting that they participate in related functions involving morphogenesis. In support of this, *tsl6-1* was identified as an allele of the nonessential gene *SLT2* or *MPK1* whose product is a MAP kinase regulating cell wall synthesis. These results indicate that this synthetic lethality approach provides a sensitive screen for the isolation of mutations affecting morphogenesis, many of which are likely to be in nonessential genes, like *BEM2* and *SLT2*.

DURING vegetative growth, *Saccharomyces cerevisiae* selects a site on its surface for bud emergence, which then directs the assembly of a polarized F-actin cytoskeleton (ADAMS and PRINGLE 1984; KILMARTIN and ADAMS 1984). The establishment of polarity in turn polarizes the secretory apparatus for appropriate cell surface expansion (reviewed in BRETSCHER *et al.* 1994). The polarized distribution of actin is modified as needed during the cell cycle to target secretion such that an appropriately shaped bud assembles and separates from the mother cell after cytokinesis (reviewed in DRUBIN and NELSON 1996). Defects in the regulation or in components of the actin cytoskeleton itself result in morphological abnormalities. Thus, yeast provides a useful system to study the establishment of polarity and how that polarity regulates the microfilament organization, which in turn determines the sites for cell growth.

S. cerevisiae has a single essential gene encoding conventional actin *ACT1* (SHORTLE *et al* 1982). Associated with the F-actin are a wealth of proteins that regulate its structure and localization (WELCH *et al.* 1994), as well as molecular motors that presumably interact with it for force generation and intracellular motility (BROWN 1997). Work over the last few years has implicated the actin cytoskeleton not only in polarized secretion during the cell cycle, but also in bud site selection (ROEMER *et al.* 1996; YANG *et al.* 1997), shmoo formation during mating (FORD and PRINGLE 1986; GEHRUNG and SNYDER 1990), receptor-mediated and fluid phase endocytosis (KUBLER and RIEZMAN 1993; GELI and RIEZMAN 1996; GOODSON *et al.* 1996), organelle segregation (SIMON *et al.* 1995; HILL *et al.* 1996), and even control of localized gene expression (BOBOLA *et al.* 1996; JANSEN *et al.* 1996).

Since actin is certain to be necessary for many essential processes, we chose to study yeast tropomyosins, as these well-studied actin-binding proteins are likely to be involved in a subset of functions that should be easier to study. Tropomyosin is necessary for viability in yeast, and this essential function can be provided by either of two genes, *TPM1* or *TPM2* (DREES *et al.* 1995). One avenue to the identification of components that are important for each tropomyosin's function is to use genetic screens for mutations that are lethal only in the absence of each isoform. Synthetic lethality screens have been used very successfully for the identification of interacting components in the yeast secretory pathway (*e.g.*, SALIMINEN and NOVICK 1987; KAISER and SCHEKMAN 1990), as well as for the identification of additional regulatory and structural components of the yeast actin cytoskeleton (*e.g.*, BENDER and PRINGLE 1991; LIU and BRETSCHER 1992; ADAMS *et al.* 1993; KARPOVA *et al.* 1993; HOLTZMAN *et al.* 1993; GOODSON *et al.* 1996; HAARER *et al.* 1996).

We recently described the use of such a screen to identify mutations that cause lethality in the absence of

Corresponding author: Anthony Bretscher, Section of Biochemistry, Molecular and Cell Biology, Biotechnology Building, Cornell University, Ithaca, NY 14853. E-mail: apb5@cornell.edu

Tpm1p (WANG and BRETSCHER 1995), the major tropomyosin isoform that is specifically associated with actin cables in the yeast cytoskeleton (LIU and BRETSCHER 1989a,b; DREES *et al.* 1995). We identified seven independent mutations that lay in six complementation groups (*tsl1-6*; tropomyosin synthetic lethal). Only one of these mutations (*tsl1-1*) conferred a temperature-sensitive phenotype in an otherwise wild-type background. The recessive conditional nature of this mutation enabled us to clone the gene by complementation, which resided in *BEM2*, a gene that encodes a *rho*-GAP (WANG and BRETSCHER 1995). Further genetic studies supported the hypothesis that Bem2p, and its probable target Rho1p, regulate microfilament structure and function in yeast (WANG and BRETSCHER 1995). However, since only one gene was identified twice, and no mutations were recovered in genes already known to show synthetic lethality with *tpm1Δ* (such as *MYO2* and *TPM2*), we were clearly far from saturating the screen. Moreover, since loss of Tpm1p itself in some backgrounds slows the growth of yeast, resulting in a longer generation time and in an aberrant actin cytoskeleton (LIU and BRETSCHER 1989, 1992), we were concerned about the specificity of the screen and whether the other *tsl* mutations were relevant to actin structure and function in yeast. The finding that *tpm1Δ* does not show general synthetic lethality with a number of irrelevant conditional lethal mutations and that the *tsl* mutations all give rise to abnormal cell morphologies (WANG and BRETSCHER 1995) suggested that they might affect the regulation and function of the actin cytoskeleton. Here we examine the phenotypes of, and the genetic interactions between, *tsl* mutations. Our analysis leads us to the conclusion that the screen provides a genetic approach to the identification of genes affecting the regulation and function of the actin cytoskeleton, many of which probably lie in nonessential genes. Thus, further exploitation of this screen may be a fruitful approach for the identification of known as well as new genes affecting morphogenesis and the actin cytoskeleton.

MATERIALS AND METHODS

Yeast strains and media: Yeast strains used in this study are listed in Table 1. Standard YPD, SD, and SC media for growing yeast are described by SHERMAN *et al.* (1991). Transformation of yeast was performed by the lithium acetate method (ITO *et al.* 1983) or using the Frozen-EZ Yeast Transformation Kit (ZYMO Research, Orange, CA). Colony sectoring assays were based on the fact that *ade2* strains accumulate a red pigment whose synthesis can be blocked by a mutation in the *ADE3* gene. Thus, an *ade2 ade3* strain with a plasmid harboring *ADE3* gene will give rise to red colonies with white sectors on nonselective media. Enhancement of the red color conferred by *ade2* was achieved by adding one-fifth the amount of adenine (1 mg/100 ml) to SD media.

Strains that were used to clone *TSL2, TSL3, TSL5,* and *TSL6* were generated as follows: ABY924 and ABY925 were transformed with the *Sac*I cut marker switching plasmid pUC4-*ura3::TRP1* and transformants were selected on SC-Trp plates to generate strains ABY600a and ABY600b. Both strains were Ura$^-$ and lacked tropomyosin I as determined by immunoblots with tropomyosin antibodies. Appropriate mating types were then mated to each *tsl* strain (ABY250, ABY251, ABY602, and ABY603), each harboring pDS1-*TPM1* (WANG and BRETSCHER 1995). Diploid cells were selected on SC-Trp-Ura and sporulated. Tetrad analyses confirmed that *tpm1Δ::ura3::TRP1* segregates away from *tpm1Δ::LEU2*, and cells that have a genotype of *tsl tpm1Δ::ura3::TRP1 ade2 ade3 ura3 leu2* can only be recovered if they harbor the pDS1-*TPM1* plasmid, which renders colonies red and the cells 5-FOA sensitive. These strains were named as ABY600-10-1a (*tsl2-2*), ABY600-22-3-13 (*tsl3-1*), ABY600-50b-b (*tsl5-1*), and ABY600-61a-27 (*tsl6-1*), respectively. These strains were used to clone the *TSL* genes by colony sectoring using a *LEU2* marker-based yeast genomic library.

Construction of a bacterial library of yeast genomic DNA: The pRS315 plasmid (SIKOSKI and HIETER 1989) was used for constructing two yeast genomic libraries, one designed with inserts of 6–9 kilobases (kb), and one with 7–12-kb inserts. The protocol was provided with a modification of that used by P. WANG and T. HUFFAKER (personal communication). Yeast genomic DNA was isolated with minimum shearing. Five hundred micrograms of DNA was partially digested with *Sau*3A to give maximal DNA staining in either 6–9- or 7–12-kb regions. The appropriately sized fragments were excised after electrophoresis and electroeluted using dialysis tubing. DNA was then phenol/chloroform extracted twice, ethanol precipitated, and resuspend in 60 μl water. Quantitation of sized fragments was done by comparison with a dilution series of λ DNA standard. pRS315 vector was digested with *Bam*HI and treated with alkaline phosphatase before being subjected to electrophoresis, elution, and ethanol precipitation as above. To set up the ligation, 200 ng of 6–9-kb and 400 ng of 7–12-kb genomic inserts were added to 100 and 75 ng vector, respectively, and ligation was performed at 16° overnight. The ligation mix was ethanol precipitated and resuspended in 10 μl TE buffer and stored at −20°. ElectroMAX DH10B cells (GIBCO BRL, Gaithersburg, MD) were transformed by electroporation and a pool of 40,000–50,000 colonies were recovered for each sized library. The 6–9-kb library yielded 85% white colonies and 83% of those white colonies had inserts. The 7–12-kb library yielded 85% white colonies and 80% of those white colonies had inserts that are greater than 7 kb.

Genetic analyses: Synthetic interactions between *tsl* mutations were performed by crossing them pairwise. *tsl2-2* (ABY661 and ABY666), *tsl3-1* (ABY662 and ABY669), *tsl5-1* (ABY663 and ABY664), and *tsl6-1*(ABY665) are segregants from backcrosses of *tsl2-2* (ABY250), *tsl3-1* (ABY251), *tsl5-1* (ABY602), and *tsl6-1* (ABY603) to ABY153 or ABY154, respectively. In all genetic analyses performed, *tsl* alleles were monitored through their distinct morphological appearances except for *bem2-10* (*ts1-1*) or *bem2Δ::LEU2*, which is Ts$^-$. For example, *tsl2-2* cells are enormous; *tsl3-1* gives multibranched cells connected like chains; *tsl5-1* has heterogeneous-sized cells with some chained cells; and, finally, *tsl6-1* cells are larger and a high percentage of cells are dead (~20% in early log phase culture when at least 200 cells were counted) marked by wrinkled cell wall (see Figure 5B).

Cloning of *TSL*s: ABY600-10-1a, ABY600-22-3-13, ABY600-50b-b, and ABY600-61a-27 were transformed with both libraries (6–9- and 7–12-kb) and a minimum of 10,000 colonies were screened for sectoring after 5–7 days incubation at room temperature. ABY600-22-3-13 and ABY600-10-1a produce some white colonies before and after transformation, possibly resulting from turning into petites. The colonies remain 5-FOA sensitive unless cells are transformed with pRS315-*TPM1*.

TABLE 1

Yeast strains used in this study

Strain	Genotype	Source
ABY164	*MATa ura3-52 leu2-3,112 his3Δ-200 lys2-801*	T. HUFFAKER, Cornell Univ.
ABY165	*MATα ura3-52 leu2-3,112 his3Δ-200 lys2-801 ade2-101*	T. HUFFAKER, Cornell Univ.
ABY248	*MATα bem2-10 ura3-52 leu2-3,112 ade2-101 ade3*	WANG and BRETSCHER (1995)
ABY249	*MATa bem2-10 ura3-52 leu2-3,112 lys2-801 ade2-101 ade3*	WANG and BRETSCHER (1995)
ABY250	*MATα tsl2-2 ura3-52 leu2-3,112 lys2-801 ade2-101 ade3*	WANG and BRETSCHER (1995)
ABY251	*MATa tsl3-1 ura3-52 leu2-3,112 lys2-801 ade2-101 ade3*	WANG and BRETSCHER (1995)
ABY602	*MATα tsl5-1 ura3-52 leu2-3,112 lys2-801 ade2-101 ade3*	WANG and BRETSCHER (1995)
ABY603	*MATα tsl6-1 ura3-52 leu2-3,112 lys2-801 ade2-101*	WANG and BRETSCHER (1995)
ABY611	*MATα ura3-52 leu2-3,112 his3Δ-200 lys2-801 ade2-101 bem2Δ::LEU2*	WANG and BRETSCHER (1995)
ABY612	*MATa ura3-52 leu2-3,112 his3Δ-200 ade2-101 trp1-1(am) bem2Δ::LEU2*	WANG and BRETSCHER (1995)
ABY168	*MATa ura3-52 leu2-3,112 his3Δ-200 lys2-801 tpm1Δ::LEU2*	LIU and BRETSCHER (1992)
ABY167	*MATα ura3-52 leu2-3,112 his3Δ-200 lys2-801 tpm1Δ::LEU2*	LIU and BRETSCHER, 1992
ABY187	*MATα ura3-52 leu2-3,112 his3Δ-200 ade2-101 trp1 myo1::LEU2*	WATTS *et al.* (1987)
ABY153	*MATα met4*	B. TYE, Cornell Univ.
ABY154	*MATa met4*	B. TYE, Cornell Univ.
ABY661	*MATα ura3-52 lys2-801 tsl2-2* Segregant of ABY250XABY154	This study
ABY666	*MATa ade2-101 his3 leu2 tsl2-2* Segregant of ABY250XABY154	This study
ABY662	*MATa lys2-801 leu2-3,112 tsl3-1* Segregant of ABY251XABY153	This study
ABY669	*MATα ura-52 ade2-101 his3 tsl3-1* Segregant of ABY251XABY153	This study
ABY663	*MATα ade2-101 his3 tsl5-1* Segregant of ABY602XABY154	This study
ABY664	*MATa ura3-52 ade2-101 tsl5-1* Segregant of ABY602XABY154	This study
ABY665	*MATa ade2-101 tsl6-1* Segregant of ABY603XABY154	This study
ABY924	*MATα ade2-101 ade3 ura3-52 leu2-3, 112 his7 trp1-1(am) tpm1Δ::URA3*	D. PRUYNE
ABY926	*MATa ade2-101 ade3 ura3-52 leu2-3, 112 his7 trp1-1(am) tpm1Δ::URA3*	D. PRUYNE
ABY600a	*MATα ade2-101 ade3 ura3-52 leu2-3, 112 his7 trp1-1(am) tpm1Δ::ura3::TRP1*	This study
ABY600b	*MATa ade2-101 ade3 ura3-52 leu2-3, 112 his7 trp1-1(am) tpm1Δ::ura3::TRP1*	This study
ABY600-10-1a	*MATα tsl2-2 ura3-52 leu2-3,112 ade2-101 ade3 tpm1Δ::ura3::TRP1*/pDS1-*TPM1* Segregant of ABY250XABY600b	This study
ABY600-22-3-13	*MATα tsl3-1 ura3-52 leu2-3,112 ade2-101 ade3 tpm1Δ::ura3::TRP1*/pDS1-*TPM1* Segregant of ABY251XABY600a	This study
ABY600-50b-b	*MATα tsl5-1 ura3-52 leu2-3,112 ade2-101 ade3 tpm1Δ::ura3::TRP1*/pDS1-*TPM1* Segregant of ABY602XABY600b	This study
ABY600-61a-27	*MATa tsl6-1 ura3-52 leu2-3,112 ade2-101 ade3 tpm1Δ::ura3::TRP1*/pDS1-*TPM1* Segregant of ABY603XABY600b	This study

This problem complicates screening for sectoring colonies. For each transformation, fresh cells were streaked out from −70° stocks and used only once. After transformation, white and particularly slow sectoring colonies were selected. Of those clones selected, plasmids carrying *TPM1* and *TPM2* were recovered numerous times, yet *TSL2*, *TSL3*, and *TSL5* remain to be identified.

Isolation and identification of *SLT2* as *TSL6*: ABY600-61a-27 was transformed with the pRS315 based 6–9- and 7–12-kb libraries, and a total of 50,000 colonies were screened in one experiment. Twenty-two potential sectoring or white colonies that are 5-FOA resistant were recovered initially and they were inoculated to either YPD media for protein extraction and Western analysis using Tpm1p antibodies or to SC-Leu media for plasmid DNA extraction and transformation of *Escherichia coli* cells to recover the plasmids. Western blots suggested that four of the plasmids contain the *TPM1* gene. Upon restriction digest analysis, 14 of them do not contain any inserts (they likely resulted from multiple plasmids co-residing in the cell and the plasmids containing the inserts were lost during plasmid recovery). The remaining four plasmids have inserts that range from 6 to 11 kb, share multiple restriction fragments with different sets of restriction digests, and do not contain any diagnostic fragments within or adjacent to the *TPM2* gene. Sequencing of the smallest insert reveals a 6365-base pair fragment on chromosome VIII containing three open reading frames (ORFs): *SLT2*, *DAP2*, and a hypothetical protein. This plasmid was named pRS315-61a-27. Subclones of an *ApaI-ApaI* fragment (3.8 kb containing *DAP2*), a *StuI-XbaI* fragment (2.7 kb containing the hypothetical ORF), and religation of plasmid after releasing the *ApaI-ApaI* fragment (2.5 kb containing *SLT2*), were retransformed into ABY918-61a-27 along with pRS315 and pRS315-*TPM1* as negative and positive controls. Only pRS315-*SLT2* and

pRS315-*TPM1* permitted the cells to sector and become 5-FOA resistant.

Plasmid constructs: pDS1-*TPM1* and pSL009 (carrying *BEM2*) have been described (WANG and BRETSCHER 1995). pRS315-*TPM1* was constructed by subcloning a *Sal*I-*Sal*I fragment of the *TPM1* gene from pDS1-*TPM1* into the pRS315 vector. pRS315-*TPM2* used in this study was recovered during attempts to clone *TSL2*. One insert was sequenced and comprises a segment of chromosome IX from 88,001 to 90,855 (2.85 kb); another is ~6.5 kb and was not sequenced, but its identity was confirmed by restriction digest and Southern blot analyses. pRS315-*SLT2* is a subclone of pRS315-61a-27 in which a 3.8-kb *Apa*I-*Apa*I fragment was deleted and only contains the *SLT2* ORF (see above and Figure 5A).

Mating factor secretion by halo assays: Wild-type and *tsl* cells of either mating type were resuspended in water at a concentration of $1-5 \times 10^6$ cells/ml. Four microliters of cells were spotted onto two gridded YPD plates and incubated at 26° for 12–16 hours. Next, $1 \times 10^4-1 \times 10^5$ *sst1* (*MAT***a**) or *sst2* (*MAT*α) cells (α- and **a**-factor tester strains; SPRAGUE 1991) were diluted in 300 to 400 μl of water and the cell mist was sprayed evenly onto the plates using a spray-tool. Halos resulting from inhibition of tester cell growth were scored after 36–48 hours of incubation at 26°.

Microscopy and imaging: Live or fixed cells were examined with a Zeiss Axiovert 100 TV microscope. Differential interference contrast and immunofluorescence images were acquired by a RTC/CCD digital camera (Princeton Instruments, Inc., Trenton, NJ) and processed through the Metamorph Imaging System (Universal Imaging Corporation, West Chester, PA). Photographs of plates and Western blots were acquired through FOTO/Analyst Archiver (FOTODYNE Inc., Hartland, WI). All micrographs were processed and assembled using Adobe Photoshop 3.0. Immunofluorescence microscopy of actin and chitin staining was performed as described (PRINGLE *et al.* 1989). Mitochondrial staining of live yeast cells was done using 3,3′dihexyloxacarbocyanine (DiOC6) (Molecular Probes, Eugene, OR) at a final concentration of 100 nM (SIMON *et al.* 1995), and vacuoles were visualized by staining live cells with N-(3-triethylammoniumpropyl)-4-(p-diethylaminophenylhexatrienyl) pyridium dibromide (FM 4-64) (Molecular Probes, Eugene, OR) according to VIDA and EMR (1995). Fluid-phase endocytosis was assayed as described by REIZMAN (1985) using Lucifer Yellow CH (Molecular Probes, Eugene, OR).

RESULTS

Phenotypic characterization of the *tsl* mutants: The screen for mutations synthetically lethal with *tpm1*Δ, using a plasmid-loss sectoring assay, has been described. Seven mutations in six complementation groups were identified and a brief description of each mutant was reported (WANG and BRETSCHER 1995). Here we characterize the *tsl* mutants in more detail (Figures 1 and 2).

Each mutant has a distinct phenotype: *bem2-10* (*tsl1-1*) is temperature sensitive and has enlarged cells with huge vacuoles; *tsl2-2* cells are very large; the *tsl3-1* mutation confers a cold-sensitive phenotype at 12° and a defect in cytokinesis resulting in multibranched and chained groups of cells; the *tsl5-1* morphological defect is relatively mild except for some big cells and a small percentage of cell populations (2% to 5%) form into chains; and *tsl6-1* cells are heterogeneous in cell size

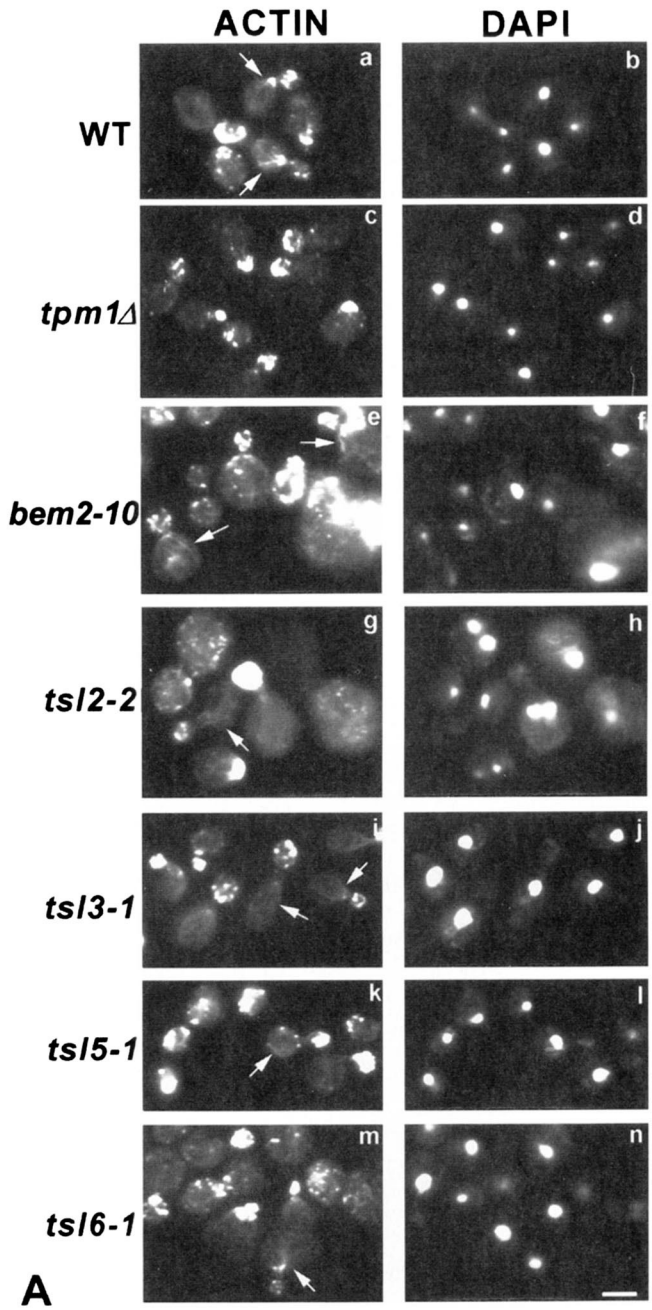

FIGURE 1.—Phenotypic analysis of *tsl* mutants. (A) Wild-type (ABY164), *tpm1*Δ (ABY167), *bem2-10* (ABY249), *tsl2-2* (ABY250), *tsl3-1* (ABY251), *tsl5-1* (ABY602), and *tsl6-1* (ABY603) cells were fixed and stained for actin with actin antibodies (a, c, e, g, i, k, and m in A) and for DNA by DAPI (b, d, f, h, j, l, and n in A). *tsl* mutant cells were selected for optimal actin staining; arrows indicate actin cables in wild-type and *tsl* mutant cells. The DIC images shown in B more accurately represent the abnormal morphology of the *tsl* mutants. Fluorescence images of mitochondria, vacuoles, and fluid-phase endocytosis were examined in the above cells after staining with $DiOC_6$ (B), FM4-64 (C), and LY-CH (D), respectively. Arrows in D denote the accumulation of LY-CH in the plasma membrane of *bem2-10*. Bars, 5 μm.

with ~20% of the early log phase cells appearing to be lysed (see also Figure 5B). In addition, *tsl2-2*, *tsl3-1*, and *tsl5-1* mutants confer an extended bud neck phenotype

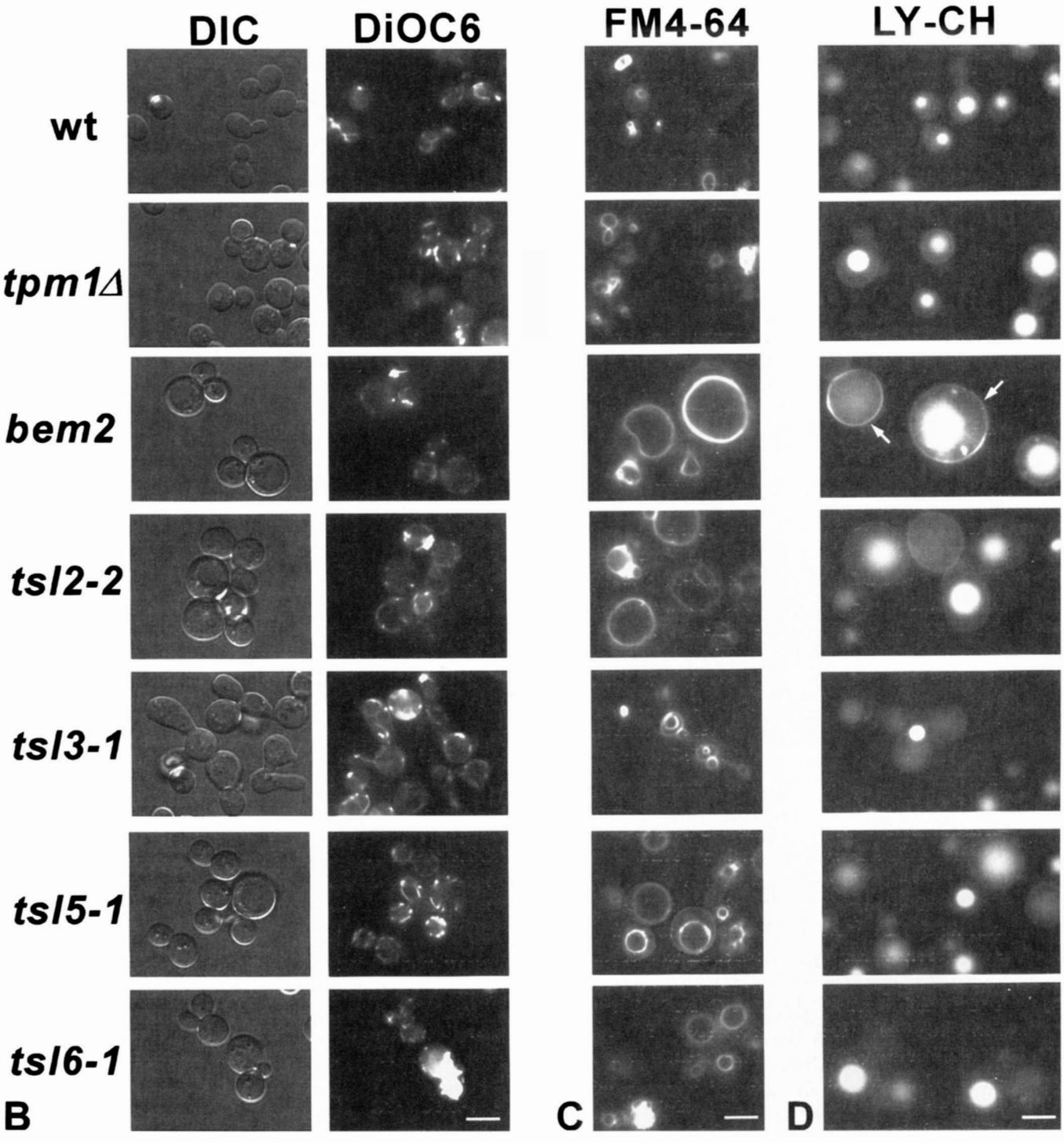

FIGURE 1.—*Continued*

and this morphological defect is also seen in the conditional *myo2-66* and *tpm1-2* mutants after shifting to the restrictive temperature (T. WANG and A. BRETCHER, unpublished data; D. PRUYNE and A. BRETCHER, personal communication). Importantly, the morphological and growth defects segregate 2:2 for each *tsl* mutant, and co-segregate with the synthetic-lethal phenotype in multiple tetrads (WANG and BRETSCHER 1995). The morphological defects are similar to those seen in cells defective in the regulation of, or in components of, microfilaments, suggesting that the *tsl* mutations might affect directly or indirectly the organization of the actin cytoskeleton. Since defects in the cytoskeleton can lead to not only an abnormal actin distribution, but also to defects in endocytosis, secretion, and organelle inheritance, this prompted us to characterize these processes in the *tsl* mutants.

Organization of the actin cytoskeleton in the tsl mutants:

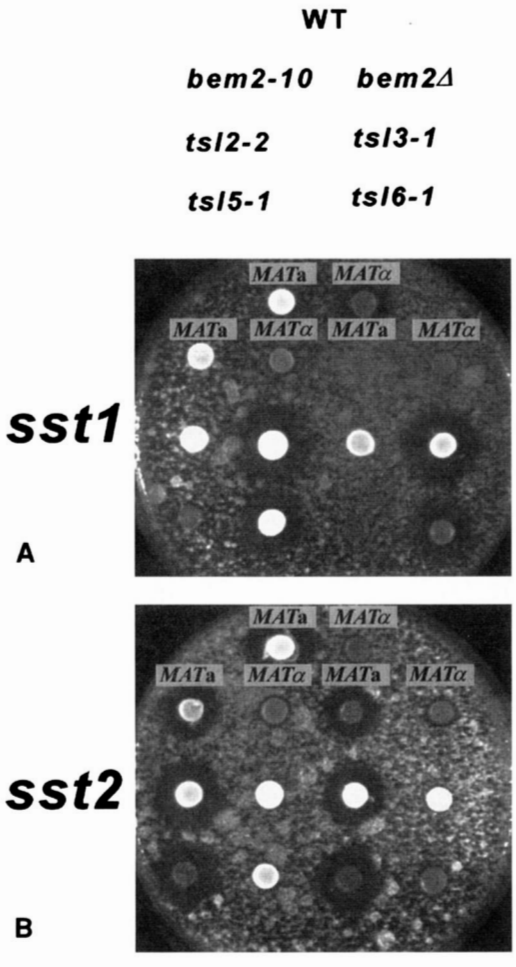

FIGURE 2.—*tsl* mutants are not defective in secretion. Secretion of yeast α- and **a**-factors were tested by halo assays using pheromone-sensitive strains, *sst1* (α tester) and *sst2* (**a** tester). Both mating types of wild-type (ABY165, ABY164), *bem2-10* (ABY248, ABY249), *bem2*Δ (ABY611, ABY612), *tsl2-2* (ABY250, ABY666), *tsl3-1* (ABY669, ABY251), *tsl5-1* (ABY602, ABY664), and *tsl6-1* (ABY603, ABY665) cells were spotted onto YPD plates before mists of *sst1* (A) and *sst2* (B) cells were sprayed. Halos produced by zones of growth inhibition were scored after 2–3 days incubation at 26°. The top diagram shows the arrangement of testing cells spotted on the YPD plates with one spot of each mating type present for each strain.

The localization of actin by immunofluorescence microscopy was determined for each strain (Figure 1A). In comparison with wild-type cells, which have polarized cortical patches and abundant actin cables, *tpm1*Δ cells have less well polarized cortical patches and no detectable actin cables (Figure 1, A and C; see also LIU and BRETSCHER 1989a, 1992). Actin cables can be seen in all the *tsl* mutants (Figure 1, arrows in e, g, i, k, and m), and these mutant cells seem to have a somewhat compromised actin cytoskeleton. Like *tpm1*Δ cells, cortical patches are delocalized in abnormally enlarged cells for each mutant, and examples seen here are *bem2-10* and *tsl2-2* (Figure 1, e and g). However, for cells having normal morphological appearances, the actin cortical dots are well localized (Figure 1, i, k, and m). We have also analyzed chitin distribution in these mutants by staining with calcoflour, since delocalized deposition of chitin is often seen in mutants defective in the actin cytoskeleton. The results for each *tsl* mutant are consistent with those of cytoskeletal mutants (data not shown), in which delocalized chitin is only observed in abnormally enlarged cells, and chitin is normally localized and restricted to the bud scar or bud neck region in normal-sized or small-budded cells.

Nuclear segregation in tsl mutants: Nuclear segregation defects are seen in cytoskeletal mutants, such as *act1*, *pfy1*Δ, and *myo2-66* (HAARER *et al.* 1993; JOHNSTON *et al.* 1991; PALMER *et al.* 1992) and mutants of signaling molecules that control actin assembly, such as *cdc42*, *cdc24*, *bem1*, and *bem2-10* (ADAMS *et al.* 1990; BENDER and PRINGLE 1991; CHAN and BOTSTEIN 1993; KIM *et al.* 1994; WANG and BRETSCHER 1995). Nuclear segregation of *tsl* mutants was monitored by DAPI staining and at least 200 cells were quantified (Figure 1A). *tsl3-1* and *tsl5-1* cells do not have any defects in nuclear segregation at 25°, but a small percentage of *tpm1*Δ and *tsl6-1* cells (4% and 5%, respectively) and a larger percentage of *bem2-10* and *tsl2-2* cells (20 and 12%, respectively) have bi- or multinucleated cells (Figure 1A, b, d, f, h, j, l, and n), indicating that these mutations impair nuclear migration.

Organelle localization and segregation: Yeast organelles such as mitochondria and vacuoles are inherited by transporting a portion of their material from the mother to the developing daughter cell during cell division. Both mitochondrial and vacuolar movement are thought to depend on actin-based motility. Yeast mitochondria and vacuoles have been shown to co-localize with actin cables (DRUBIN *et al.* 1993; HILL *et al.* 1996). A specific mutation in the *ACT1* gene (*act1-133*) results in aggregation of mitochondria and impairment of their movement (SIMON *et al.* 1995). Similarly, vacuolar inheritance is defective in a variety of actin mutants and in the *myo2-66* mutant (HILL *et al.* 1996). To probe whether the *tsl* mutants are impaired in organelle location or movement, we determined the location of mitochondria and vacuoles in each *tsl* mutant (Figure 1, B and C). Neither *tpm1*Δ nor any of the *tsl* mutants has any detectable defects in the location of mitochondria or vacuoles. In every small-budded cell, the bud stains positively for mitochondrial or vacuolar materials, indicating normal segregation. However, subtle differences in staining of these cells were observed. *tsl2-2* and *tsl6-1* cells generally have weaker fluorescence signals by DiOC6 compared to others and the staining was not uniform throughout the population, which may be a result of strain differences in dye uptake. These results suggest that *tsl* mutations do not seem to interfere with organelle location and segregation. However, it is possible that more subtle defects in organelle segregation are not detected by these methods. For example, *tpm1*Δ cells become petite at high frequency (LIU and

BRETSCHER 1989a), perhaps due to a reduced efficiency of mitochondrial segregation and thereby an increased frequency of daughter cells inheriting mitochondria lacking DNA.

tsl mutants do not have a general defect in secretion or fluid-phase endocytosis: Previous results have suggested that Tpm1p might be involved in targeting of specific secretory materials required for cell growth, rather than having a general defect in secretion (LIU and BRETSCHER 1992; see BRETSCHER *et al.* 1994 for review). Thus, polarized cell secretion is partially impaired in *tpm1*Δ cells resulting in excessive isotropic growth and the generation of enlarged rounded cells. Similar observations have also been made for other cytoskeletal mutants such as *myo2-66* (GOVINDAN *et al.* 1995). The abnormally enlarged cells observed in *tsl* mutants also suggest a defect in polarized cell growth. To investigate whether *tsl* mutants have a general defect in secretion, we analyzed the efficiency of α-factor secretion. Yeast *MAT*α cells produce α-factor through the normal secretory pathway whereas *MAT***a** cells secrete **a**-factor through a special transporter in the plasma membrane (MICHAELIS 1994). Strains bearing mutations in *sst1* and *sst2* are supersensitive to the α- and **a**-factor mating pheromones, respectively, and can be used to detect the amount of mating pheromone released from tester cells by the size of the halo, which indicates the zone of growth inhibition. As expected, *tpm1*Δ and *tsl* cells produce normal **a**-factor, as indicated by a zone of growth inhibition of *sst2* cells (Figure 2B). Importantly, α-factor secretion is also normal in *tpm1*Δ and most *tsl* mutants by the halo assay, but not for *bem2-10* (*tsl1-1*) and *bem2*Δ (Figure 2A). The small or undetectable halos produced by *MAT*α *bem2* mutants are reproducible and raise the question whether Bem2p is directly involved in secretion. Two lines of evidence suggest that Bem2p does not affect secretion directly. First, invertase does not accumulate in *bem2* cells and the processing of the vacuolar enzyme carboxypeptidase Y is normal (data not shown). Second, Western blots with antibodies to α-factor reveal that mature α-factor is secreted into the medium from *bem2* cells and there is no abnormal accumulation of α-factor precursors in total cell extracts. As a result, the small or undetectable halos produced by *bem2* mutants are probably due to a low rate of α-factor synthesis. Thus, we conclude that, like *tpm1*Δ cells, *bem2* and other *tsl* mutants do not have a general secretory defect, at least as assayed by α-factor secretion. However, the possibility still remains that they may affect the kinetics and targeting of secretory components.

Some components of the actin cytoskeleton play a role in endocytosis. For example, receptor-mediated endocytosis depends on actin and fimbrin (KUBLER and RIEZMAN 1993) and a mutant isolated on the basis of a defect in endocytosis, *end4*, is an allele of *SLA2*, which is believed to be a cytoskeletal protein. Recently, the myosins I encoded by *MYO3* and *MYO5* have also been demonstrated to play a role in receptor-mediated and fluid-phase endocytosis (GELI and RIEZMAN 1996; GOODSON *et al.* 1996). To find out whether *TSL* gene products are required for endocytosis, we have examined the *tsl* mutants for their ability to take up lucifer yellow (LY-CH) as a endocytic marker (REIZMAN 1985). LY-CH accumulated inside the vacuoles in *tpm1*Δ, *tsl2-2*, *tsl3-1*, *tsl5-1*, and *tsl6-1* cells, suggesting a normal endocytic process. However, in addition to vacuolar staining, plasma membrane staining was also observed in *bem2-10* cells, especially in abnormally enlarged cells (Figure 1D). Thus, the *bem2* mutation might cause a reduced endocytic rate, rather than a complete block in fluid-phase endocytosis. In conclusion, *tsl* and *tpm1*Δ cells do not have a general defect in either secretion or fluid-phase endocytosis.

Genetic interactions between *tsl* mutations: *Synthetic interactions between tsl mutations:* Since *tsl* mutants were isolated by their synthetic interactions with *tpm1*Δ, it is likely that the products of the *TSL* genes are also functionally related. To test whether *tsl* mutations interact with each other genetically, we have crossed all haploid mutants pairwise and analyzed the resulting tetrads (Table 2). Typically, 24–36 tetrads were dissected for each cross. However, due to poor spore viability, which likely results from chromosome missegregation during meiosis, the sample sizes derived from crosses involving *tsl2-2* and *tsl6-1* are quite small. Nevertheless, the data in Table 2 suggests that *TSL* genes are not linked to each other in general, however, the linkage properties for crosses between *tsl2-2* and *tsl5-1*, *tsl5-1* and *tsl6-1* may be subject to changes when more tetrads are analyzed. For nonsynthetic lethal interactions (NSL), viable spores with double mutations were recovered and no phenotypic or growth-rate changes were observed from that of single mutations upon examination under the microscope. Interestingly, *bem2* is synthetically lethal with *tsl2-2* and *tsl3-1* at 25°. Synthetic interactions, when presumptive double mutations are either dead or the recovered double mutants are extremely sick with additive morphological phenotypes and slower growth rate at 25°, were seen between *tsl3-1* and *tsl2-2* or *tsl6-1*. These results therefore suggest that *bem2*, *tsl2-2*, and *tsl3-1* participate in related pathways. Since overexpression of Bem2p does not suppress the phenotypes caused by *tsl2-2* and *tsl3-1* (data not shown), it is very unlikely that their functions are redundant. A synthetic interaction was also observed between *tsl3-1* and *tsl6-1*. The fact that *tsl6-1* shows interactions with *tsl3-1* but not *bem2* or *tsl2-2* suggest that *tsl3-1* may have more than one function involving different sets of genes. Collectively, these results suggest that *TSL* genes contribute to a set of integrated functions.

tsl5-1 and bem2 mutants exhibit noncomplementing phenotypes: Heterozygous diploids of the genotype *tpm1*Δ/*tpm1*Δ *ade2/ade2 ade3/ade3 ura3/ura3 leu2/leu2 bem2-10/*

TABLE 2

Synthetic interactions between *tsl* mutations

		PD[a]	TTP	NPD
tsl1-1 (ABY249) × *tsl2-2* (ABY661)	SL[b]	3	9	0
bem2Δ (ABY611) × *tsl3-1* (ABY662)	SL	3	13	2
bem2Δ (ABY611) × *tsl5-1* (ABY664)	Viable	4	15	1
bem2Δ (ABY611) × *tsl6-1* (ABY665)	Viable	1	8	2
tsl2-2 (ABY250) × *tsl3-1* (ABY251)	SS[c]	0	6	7
tsl2-2 (ABY250) × *tsl5-1* (ABY664)	Viable	6	7	1
tsl2-2 (ABY661) × *tsl6-1* (ABY665)	Viable	0	8	1
tsl3-1 (ABY662) × *tsl5-1* (ABY663)	Viable	2	8	2
tsl3-1 (ABY662) × *tsl6-1* (ABY603)	SS	1	16	1
tsl5-1 (ABY663) × *tsl6-1* (ABY665)	Viable	3	6	0

[a] PD, parental ditype; TTP, tetratype; NPD, nonparental ditype.
[b] SL, synthetically lethal.
[c] SS, synthetically sick: combinations that grow much less well than either parent.

BEM2 tsl5-1/TSL5 with the sectoring plasmid pDS1-*TPM1* are able to sector normally and are 5-FOA resistant, showing that *tsl5-1* and *bem2-10* complement. Surprisingly, in the presence of *TPM1* (by selecting for pDS1-*TPM1*), the morphological defect exhibited by *bem2-10* is evident in the heterozygous diploid, though not in a *bem2-10/BEM2 TSL5/TSL5* diploid, suggesting a partial noncomplementing phenotype between *bem2* and *tsl5-1*. As shown above (Table 2), *bem2* is not linked to *tsl5-1* nor do they show any synthetic growth defects: the *bem2 tsl5-1* haploid double mutant is viable and has a morphological appearance similar to the *bem2* mutant. To further characterize this phenotype, we crossed *tsl5-1* (ABY664) to *bem2Δ* (ABY611) cells (both *TPM1*$^+$) to generate the *tsl5-1/TSL5 bem2Δ/BEM2* diploid. We have also examined whether an extra copy of *BEM2* could suppress the morphological defect exhibited by the heterozygous diploid. The mating specificities of the *tsl5-1* and *bem2Δ* haploids and *tsl5-1/TSL5 bem2Δ/BEM2* diploid were tested by complementation. As expected, the *tsl5-1* and *bem2Δ* haploid cells were able to mate with appropriate tester strains, whereas the *tsl5-1/TSL5 bem2Δ/BEM2* diploid could not (Figure 3A). *bem2Δ* confers temperature sensitivity, which is complemented by *BEM2* on a plasmid (pSL009) and *bem2Δ/BEM2 tsl5-1/TSL5* is not temperature sensitive, indicating that the temperature sensitivity conferred by *bem2* mutation is complemented (Figure 3B). However, the morphological defect exhibited by *bem2* is not complemented in *tsl5-1/TSL5 bem2Δ/BEM2* diploid cells (Figure 3C, e) but is suppressed by the presence of an extra copy of *BEM2* (Figure 3C, f). The same results were obtained when *bem2-10* was used instead of *bem2Δ*, suggesting that this noncomplementing phenotype is not allele or background dependent. As this morphological noncomplementing phenotype was not observed in heterozygotic diploids of *bem2Δ/BEM2* or *bem2Δ* crossed to other *tsl* mutants, *tsl5-1* and *bem2* have a partial noncomplementing phenotype, indicating that Tsl5p interacts with Bem2p in a dosage-dependent manner.

TPM2 is a dosage suppressor of tsl tpm1Δ mutants: In an effort to clone the *TSL2, TSL3, TSL5,* and *TSL6* genes by restoration of sectoring in transformants, we expected to recover plasmids containing *TPM1* or the *TSL* gene. However, in addition to recovering plasmids with *TPM1*, we repeatedly also recovered plasmids with *TPM2* for each *tsl* mutant. When *tsl tpm1Δ::ura3::TRP1 ura3 leu2* mutants harboring the pDS1-*TPM1* plasmid were transformed with the pRS315 vector alone, they failed to sector and were 5-FOA sensitive (Figure 4A). However, when cells were transformed with pRS315-*TPM1* or pRS315-*TPM2*, they sectored and became 5-FOA resistant. Since all the original mutants carry wild-type *TPM2* on the chromosome (see Figure 4B, lanes 3–6), the finding that an extra copy of *TPM2* could substitute for the function of *TPM1* was unexpected. It is known that *TPM1* and *TPM2* share the same essential function and the *in vivo* ratio of Tpm1p to Tpm2p is ~6:1 (DREES *et al.* 1995). Clearly, the expression of chromosomal *TPM2* is tightly regulated, as the Tpm2p levels are not changed in *tpm1Δ* alone, in *tsl tpm1Δ/*pDS1-*TPM1*, or in *tsl tpm1Δ*/pRS315-*TPM1* cells (Figure 4B, lanes 2–10). However, the expression of *TPM2* is increased three- to fivefold in *tsl tpm1Δ* cells that were transformed with pRS315-*TPM2* (Figure 4B, lanes 11–14). Because *TPM2* is a specific dosage suppressor of the lethality seen in *tsl tpm1Δ* cells, these results show that the *tsl* mutations have the common and special property of being unable to grow under conditions of low levels of either tropomyosin.

tsl6-1 is an allele of SLT2 (MPK1): In addition to the *TPM1* and *TPM2* genes, we have recovered four different but overlapping plasmids that permit the *tsl6-1 tpm1Δ* haploid with the pDS1-*TPM1* plasmid (ABY600-61a-27) to sector and become 5-FOA resistant. Sequencing, subcloning and retransformation confirm that the *SLT2* or *MPK1* is the ORF responsible (Figure 5A). *SLT2* is a MAP kinase that is activated via a kinase cascade by *PKC1*, a homologue of mammalian protein kinase C. Together, they regulate yeast cell wall synthesis

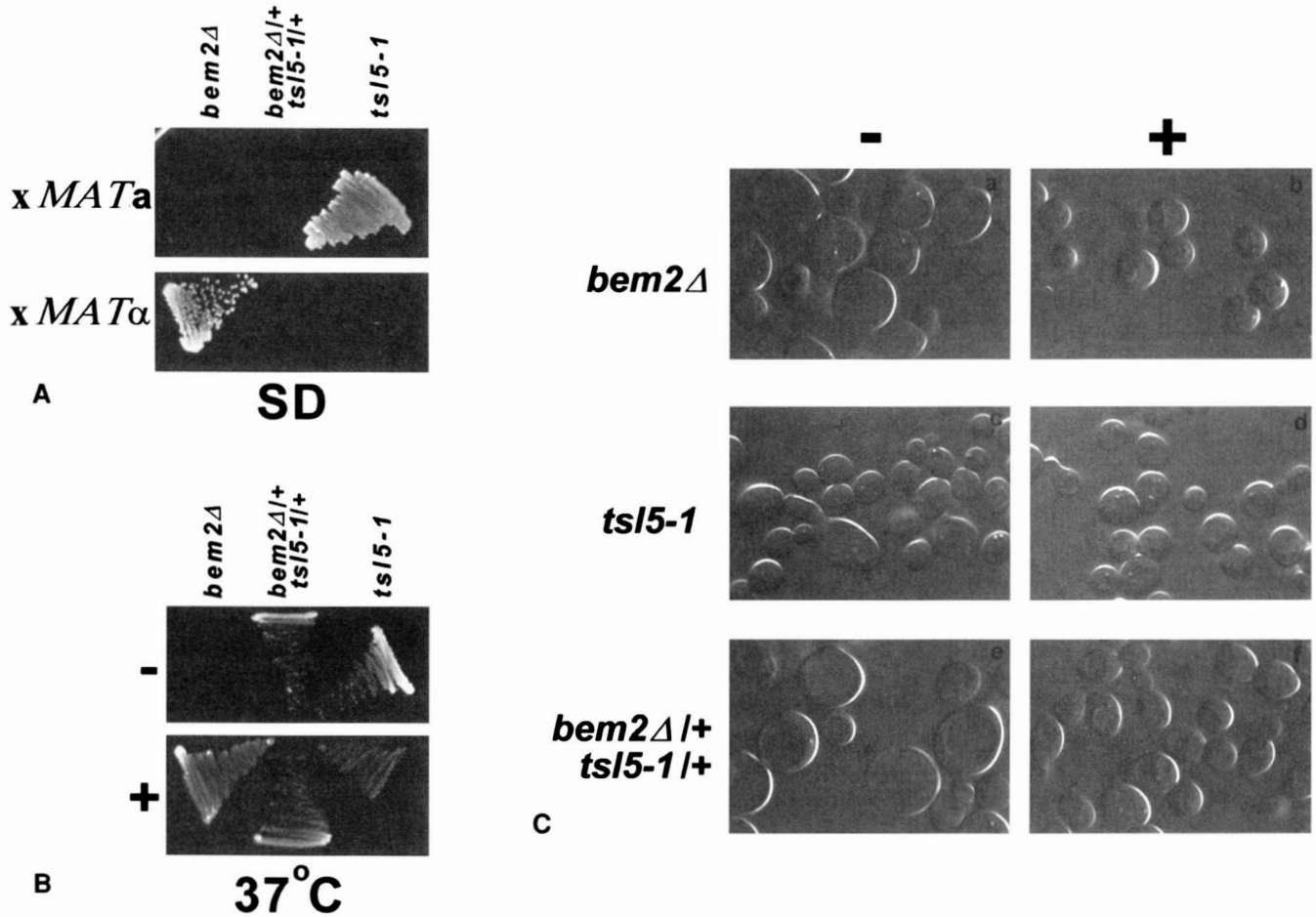

FIGURE 3.—*bem2*Δ shows morphological unlinked noncomplementation with *tsl5-1*. (A) The mating specificity of haploid *bem2*Δ (ABY611), *tsl5-1* (ABY644) cells, and heterozygotic diploid *bem2*Δ*/BEM2 tsl5-1/TSL5-1* cells were tested by nutritional auxotrophy complementation with ABY154 (*MAT*α tester) and ABY153 (*MAT***a** tester), respectively. (B) The Ts$^-$ phenotype of *bem2*Δ is complemented by *tsl5-1*. +, −, presence or absence of pSL009 carrying *BEM2* (WANG and BRETSCHER 1995). (C) The morphological defects in *bem2*Δ cells was not complemented in *bem2*Δ*/BEM2 tsl5-1/TSL5* cells (compare a and e), but can be suppressed by an extra copy of *BEM2* (f). +, −, presence or absence of pSL009 carrying *BEM2* (WANG and BRETSCHER 1995).

(see HERSKOWITZ 1995 for review). Mutations in *SLT2* cause cells to lyse, which is consistent with its role in cell wall integrity, and the cell lysis phenotype has been observed for *tsl6-1*, as noted above. To confirm that *tsl6-1* is an allele of *SLT2*, we performed linkage analyses. *tsl6-1* was crossed to *myo1::LEU2*, which is adjacent to the *SLT2* locus and tetrads from the resulting diploid were analyzed. Since only parental ditype tetrads were recovered, *tsl6-1* is closely linked to *SLT2*. Furthermore, *SLT2*, on a CEN plasmid, suppresses the morphological defects and the cell lysis phenotype of *tsl6-1*, both in early and late log phase cell cultures (Figure 5B). Therefore, *tsl6-1* resides in the *SLT2* gene.

DISCUSSION

In this article we have evaluated the phenotypic spectrum of mutations that confer inviability in the absence, but not presence, of Tpm1p. Synthetic lethal screens have been very effective in cases where loss of a gene function has conferred little or no phenotype (*e.g.*, *MSB1* or *Abp1*; BENDER and PRINGLE 1991; HOLTZMAN *et al.* 1993); however, the approach of using such a screen where loss of function of the gene under study confers poorer growth has been less generally used.

What type of mutations would one expect to show synthetic lethality with *tpm1*Δ? In the absence of Tpm1p, which is the major tropomyosin isoform in *S. cerevisiae*, cells are dependent for viability on the minor isoform, Tpm2p. There are at least two classes of mutations that one might expect to recover. The first render cells inviable due to a defect in an essential Tpm1p-dependent function for which Tpm2p cannot substitute. The second type of mutations are ones that cannot survive in a low level of either tropomyosin. Alternatively, there may be a class of mutations that make the cells generally sick (such as partial defects in protein synthesis) and in combination with the somewhat deleterious mutation, *tpm1*Δ, are inviable. There are many reasons why this last scenario is unlikely. (1) All the *tsl* mutants have a clear morphological defect in the presence of Tpm1p, indicating a defect in the regula-

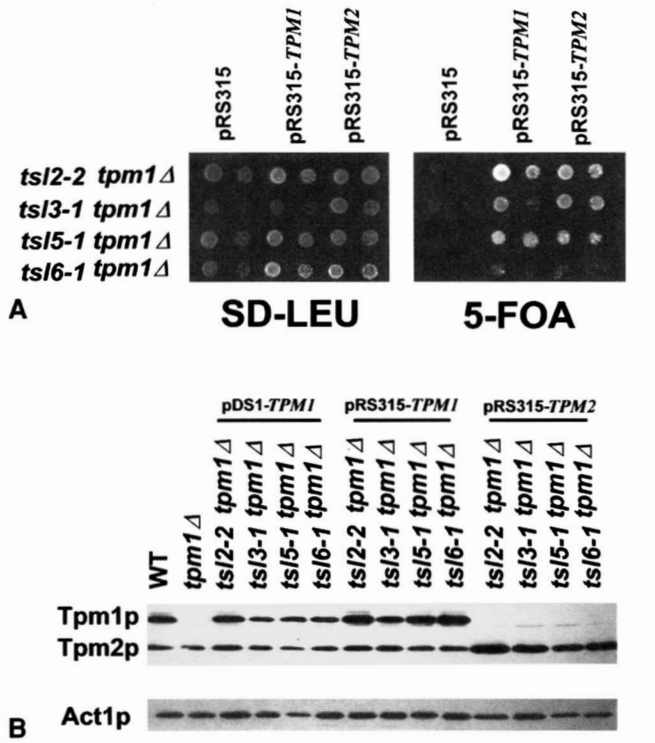

FIGURE 4.—Mutations in *TSLs* depend on the function of yeast tropomyosin. (A) The inviability of *tsl tpm1*Δ *TPM2*$^+$ cells can be suppressed by either *TPM1* or an extra copy of *TPM2*. *tsl2-2 tpm1*Δ/pDS1-*TPM1* (ABY600-10-1a), *tsl3-1 tpm1*Δ/pDS1-*TPM1* (ABY600-22-3-13), *tsl5-1 tpm1*Δ/pDS1-*TPM1* (ABY600-50b-b), and *tsl6-1 tpm1*Δ/pDS1-*TPM1* (ABY600-61a-27) cells were transformed with pRS315 (vector alone), pRS315-*TPM1*, and pRS315-*TPM2*, respectively. Dilutions of cells were spotted on either SD-LEU or 5-FOA plates. Only the cells that were transformed with *TPM1* or contain an extra copy of *TPM2* become Sect$^+$ on SD-LEU plate (not evident in the micrograph) and 5-FOA resistant. (B) Immunoblot analysis of Tpm1p and Tpm2p with an antiserum that recognizes both tropomyosin isoforms (DREES *et al.* 1995) using total cell lysates from wild-type cells (ABY164), *tpm1*Δ (ABY167), and the above *tsl tpm1*Δ strains harboring pDS1-*TPM1*, pRS315-*TPM1*, and pRS315-*TPM2*, respectively. Note that the level of Tpm2p is increased three- to fivefold (lanes 11–14) in cells harboring an extra copy of *TPM2* in comparison to wild-type (lane 1), *tpm1*Δ (lane 2), and *tsl tpm1*Δ cells containing *TPM1* plasmid (lanes 3–10). Approximately the same amounts of total proteins were loaded in each lane, as revealed by reprobing the blot with actin antibodies (Act1p). Sect$^+$ denotes sectoring cells, and quantitation of Tpm2p levels was done by comparing Western blots using twofold serial dilutions of the protein samples.

tion or structure of the microfilament cytoskeleton. (2) *tpm1*Δ cells do not show synthetic lethality with many deterious cytoskeletal mutations (see below). (3) Synthetic interactions are found among the *tsl* mutations. (4) The inviability of all the *tsl tpm1*Δ *TPM2*$^+$ combinations can be alleviated by expression of *TPM1* or a second copy of the *TPM2* gene. Thus, either Tpm1p or elevation of the level of Tpm2p can very specifically suppress the synthetic lethality. (5) At 25°, *tpm1*Δ cells in the background we used here are not that sick and extra copies of *TPM1* and *TPM2* do not make a noticeable difference in growth rate on plates. This strongly argues that the lethality lies in loss of an essential function involving either Tpm1p or Tpm2p; this is most likely the essential function of tropomyosin noted earlier (DREES *et al.* 1995).

Having established that the *tsl* mutations are specifically sensitive to low levels of tropomyosin in the cell, in what types of genes would they be expected to lie? Intuitively, we might have expected them to be in genes specifying components of the cytoskeleton. However, phenotypic analysis suggested no major cytoskeletal defects, such as loss of actin cables or defects in the localization of organelles, but did reveal some defects in nuclear segregation, which is also notable in cells defective in the regulation of the actin cytoskeleton such as *cdc42*, *cdc24*, *bem1*, and *bem2* (ADAMS *et al.* 1990; BENDER and PRINGLE 1991; CHAN and BOTSTEIN 1993; KIM *et al.* 1994; WANG and BRETSCHER 1995). Moreover, it is already known that *tpm1*Δ does not show synthetic lethality with a large number of conditional mutations in the *act1* gene or with defects in many of the components of the cytoskeleton, such as *cap1*Δ, *cap2*Δ, *sac6*Δ, *abp1*Δ, *myo1*Δ, and *myo4*Δ (ADAMS *et al.* 1993; WANG and BRETSCHER 1995). In fact, prior to our screen, the only mutations of cytoskeletal components *tpm1*Δ known to show synthetic lethality with were *tpm2*Δ and *myo2-66* (LIU and BRETSCHER 1992; DREES *et al.* 1995), which encodes yeast's only essential myosin (BROWN 1997). Given these findings, it seems that the proteins affected by the *tsl* mutations are most likely not structural components of microfilaments, but factors that regulate their structure. Indeed, both Bem2p and Slt2p (encoded by *TSL1* and *TSL6*, respectively) belong to this category. Our analysis has shown genetic interactions between a number of the *tsl* mutations (see Figure 6 for summary): *tsl1-1/bem2-10* shows synthetic lethality with *tsl2-2* and *tsl3-1*, and *tsl3-1* shows synthetic interactions with *tsl2-2* and *tsl6-1*, and the *bem2*Δ/+ *tsl5-1*/+ diploid is morphologically defective compared to the *bem2*Δ/+ and *tsl5-1*/+ diploids. This latter result indicates that the level of the Bem2p is critical to the appropriate functioning of Tsl5p or vice versa. The combined scenario from our analysis suggests that the screen has effectively isolated mutations in a group of interacting genes that control morphogenesis.

So far we have succeeded in cloning two of the *tsl* genes: *tsl1-1* lies in *BEM2*, encoding a *rho*-GAP (WANG and BRETSCHER 1995) and *tsl6-1* lies in *SLT2*, which encodes a MAP kinase. *slt2* was previously isolated as a synthetic lethal mutant with *cdc28*, a protein kinase that coordinates the cell cycle with morphogenesis by associating with specific cyclins (MAZZONI *et al.* 1993; LEW and REED 1993, 1995). MAZZONI and his colleagues have shown that actin cortical dots are grossly delocalized in the abnormally enlarged *slt2* cells and that the *slt2* mutant also shows synthetic lethal interactions with *myo2-*

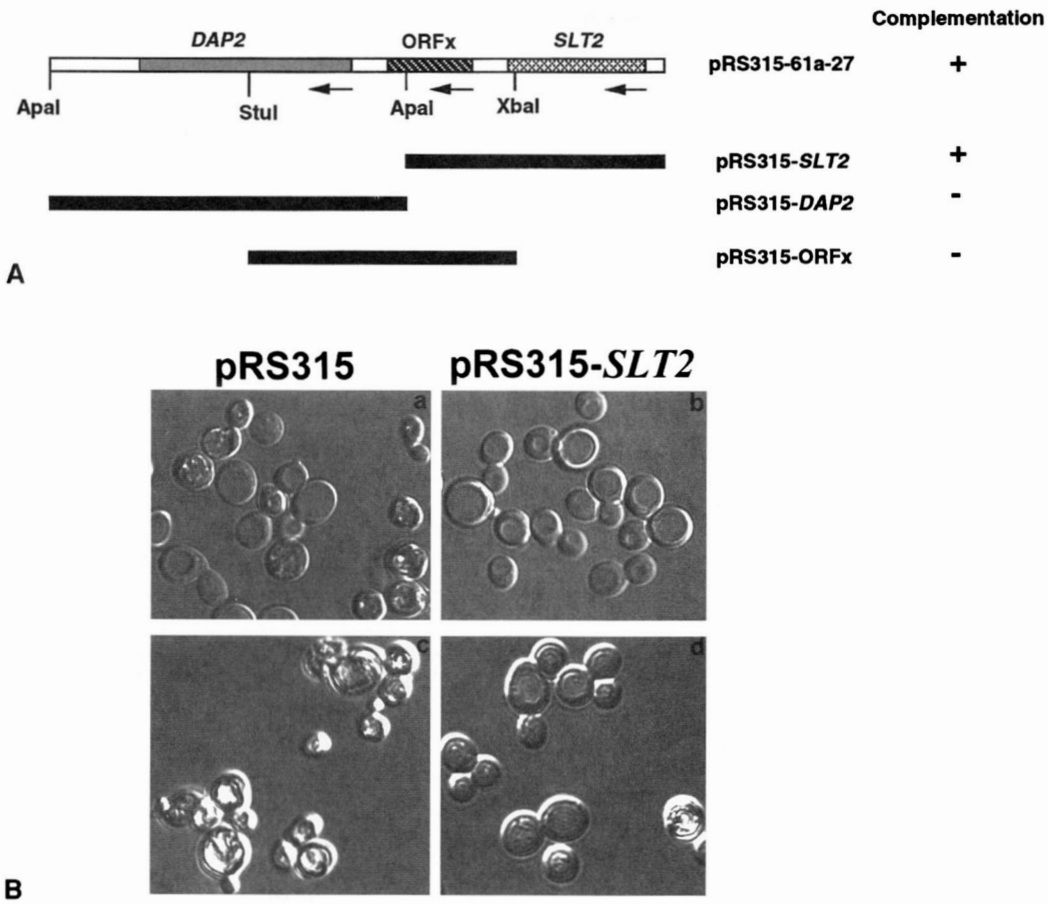

FIGURE 5.—The *tsl6-1* mutation lies in *SLT2/MPK1*. (A) The plasmid pRS315-61a-27 permits strain ABY600-61a-27 to sector and become 5-FOA resistant. It contains a 6.3-kb insert. The ability of subfragments to complement *tsl6-1* is shown with corresponding ORFs. Selected restriction sites used in cloning these subfragments are also indicated. (B) Cell lysis phenotype of *tsl6-1* (ABY603) was suppressed by pRS315-*SLT2* (b and d), but not vector alone (a and c). a and b, cells were photographed in early log phase (OD = 0.3 and 0.4, respectively). c and d, cells were photographed in late log phase (OD = 1.1 and 1.4, respectively).

66 and *act1-2*. Isolation of *slt2* as a mutant synthetically lethal with *tpm1*Δ strongly supports the idea that the functions of the actin cytoskeleton and signaling molecules involved in cell wall synthesis are well integrated. In addition to their interactions with *TPM1*, there is also a functional relationship between Bem2p and Slt2p (Figure 6). It is known that rho-related GTPases control morphogenesis by regulating the actin cytoskeleton during different stages of the cell cycle (MADAULE *et al.* 1987; ADAMS *et al.* 1990; JOHNSON and PRINGLE 1990; MATSUI and TOH-E 1992a,b; YAMOCHI *et al.* 1994). Rho1p is believed to play a role in initial bud growth by both stimulating β(1-3)-D-glucan synthase (ARELLANO *et al.* 1996; DRGONOVA *et al.* 1996; QADOTA *et al.* 1996) and activating *PKC1*, which activates the *SLT2* MAP kinase cascade (NONAKA *et al.* 1995). We and others have provided evidence that Bem2p is a specific GTPase activating protein for Rho1p (MADUALE *et al.* 1994; WANG and BRETSCHER 1995). Thus, both Bem2p and Slt2p are involved in the morphogenesis and cell wall synthesis pathways, and their functions are dependent on the integrity of actin cytoskeleton. These results therefore support the hypothesis that the *tsl* mutations in general are likely to affect regulation of the actin cytoskeleton.

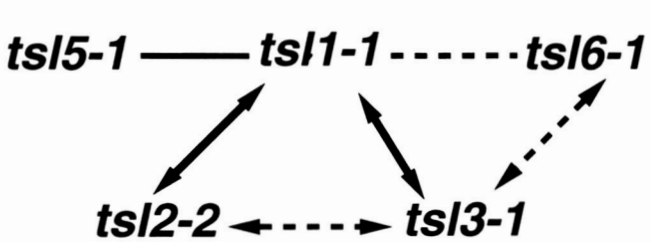

FIGURE 6.—Diagram of genetic and functional interactions between *tsl* mutations. ◄——►, synthetically lethal; ◄- - -►, synthetically sick. The morphological unlinked noncomplementing phenotype exhibited by *tsl1-1* and *tsl5-1* is indicated by a solid line, and the knowledge that *tsl1-1* (*bem2-10*) and *tsl6-1* (*slt2*) encode proteins functioning in the same pathway is indicated by a dashed line.

In summary, our data indicate that the screen for mutants that are lethal in the absence of Tpm1p result in the isolation of mutations in a variety of genes affecting morphogenesis through regulation of the actin cytoskeleton. Many of these, like *tsl6-1*, which lies in the nonessential gene *SLT2*, are likely to be in dispensable genes and therefore often missed in screens that rely on the isolation of conditional lethal mutations. The further use of this screen, and of identifying the genes in which the *tsl2-2*, *tsl3-1*, and *tsl5-1* mutations lie, should be an informative venture. Similar strategies could be applied meaningfully to other cases in which defects in a protein confer a significant growth defect. Very recently, such an approach has been successfully applied to mutant profilin (HAARER *et al.* 1996).

We thank PEIJING WANG for tips in construction of the yeast geno-

mic libraries. We also thank DAVID PRUYNE for comments on the manuscript. This work was supported by National Institutes of Health (NIH) grant GM-39066 (to A.B.) and NIH Postdoctoral Fellowship 1F32GM-17018 (to T.W.).

LITERATURE CITED

ADAMS, A. E. M., and J. R. PRINGLE, 1984 Relationship of actin and tubulin distribution to bud growth in wild-type and morphogenetic mutant *Saccharomyces cerevisiae*. J. Cell Biol. **98:** 934–945.

ADAMS, A. E. M., D. JOHNSON, R. LONGNECKER, B. SLOAT and J. R. PRINGLE, 1990 *CDC42* and *CDC43*, two additional genes involved in budding and establishment of cell polarity in the yeast *Saccharomyces cerevisiae*. J. Cell Biol. **111:** 131–142.

ADAMS, A. E. M., J. A. COOPER and D. G. DRUBIN, 1993 Unexpected combinations of null mutations in genes encoding the actin cytoskeleton are lethal in yeast. Mol. Biol. Cell **4:** 459–468.

ARELLANO, M., A. DURAN and P. PEREZ, 1996 Rho1 GTPase activates the (1-3)β-D-glucan synthase and is involved in *Schizosaccharomyces pombe* morphogenesis. EMBO J. **15:** 4584–4591.

BENDER, A., and J. R. PRINGLE, 1991 Use of a screen for synthetic lethal and multicopy suppressing mutants to identify two new genes involved in morphogenesis in *Saccharomyces cerevisiae*. Mol. Cell. Biol. **11:** 1295–1305.

BOBOLA, N., R. P. JANSEN, T. H. SHIN and K. NASMYTH, 1996 Asymmetric accumulation of Ash1p in postanaphase nuclei depends on a myosin and restricts yeast mating-type switching to mother cells. Cell **84:** 699–709.

BRETSCHER, A., B. DREES, E. HARSAY, D. SCHOTT and T. WANG, 1994 What are the basic functions of microfilaments? Insights from studies in budding yeast. J. Cell Biol. **126:** 821–825.

BROWN, S. S., 1997 Myosins in yeast. Curr. Opin. Cell Biol. **9:** 44–48.

CHAN, C. S. M., and D. BOTSTEIN, 1993 Isolation and characterization of chromosome-gain and increase-in-ploidy mutants in yeast. Genetics **135:** 677–691.

DREES, B., C. BROWN, B. G. BARRELL and A. BRETSCHER, 1995 Tropomyosin is essential in yeast, yet the *TPM1* and *TPM2* products perform distinct functions. J. Cell Biol. **128:** 383–392.

DRGONOVA. J, T. DRGON, K. TANAKA, R. KOLLER, G. C. CHEN *et al.*, 1996 Rho1p, a yeast protein at the interface between cell polarization and morphogenesis. Science **272:** 277–281.

DRUBIN, D. G., and W. J. NELSON, 1996 Origins of cell polarity. Cell **84:** 335–344.

DRUBIN, D. G., K. G. MILLER and K. F. WERTMAN, 1993 Actin structure and function: roles in mitochondria organization and morphogenesis in budding yeast and identification of the phalloidin binding site. Mol. Biol. Cell **4:** 1277–1294.

FORD, S., and J. R. PRINGLE, 1986 Development of spatial organization during the formation of zygotes and shmoos in *Saccharomyces cerevisiae* (Abstr.). Yeast **2:** S114.

GEHRUNG, S., and M. SNYDER, 1990 The *SPA2* gene of *Saccharomyces cerevisiae* is important for pheromone-induced morphogenesis and efficient mating. J. Cell Biol. **111:** 1451–1464.

GELI, M. I., and H. RIEZMAN, 1996 Role of type I myosins in receptor-mediated endocytosis in yeast. Science **272:** 533–535.

GOODSON, H. V., B. L. ANDERSON, H. M. WARICK, L. A. PON and J. A. SPUDICH, 1996 Synthetic lethality screen identifies a novel yeast myosin I gene (*MYO5*): myosin I proteins are required for polarization of the actin cytoskeleton. J. Cell Biol. **133:** 1277–1291.

GOVINDAN, B., R. BOWSER and P. NOVICK, 1995 The role of Myo2, a yeast class V myosin, in vesicular transport. J. Cell Biol. **128:** 1055–1068.

HAARER, B. K., A. S. PETZOLD and S. S. BROWN, 1993 Mutational analysis of yeast profilin. Mol. Cell. Biol. **13:** 7864–7873.

HAARER, B. K., A. CORBETT, Y. KWEON, A. S. PETZOLD, P. SILVER *et al.*, 1996 *SEC3* mutations are synthetically lethal with profilin mutations and cause defects in diploid-specific bud-site selection. Genetics **144:** 495–510.

HERSKOWITZ, I., 1995 MAP kinase pathways in yeast: for mating and more. Cell **80:** 187–197.

HILL, K. L., N. L. CATLETT and L. S. WEISMAN, 1996 Actin and myosin function in directed vacuole movement during cell division in *Sacchromyces cerevisiae*. J. Cell Biol. **135:** 1535–1549.

HOLTZMAN, D. A., S. YANG and D. G. DRUBIN, 1993 Synthetic-lethal interactions identify two novel genes, *SLA1* and *SLA2*, that control membrane cytoskeleton assembly in *Saccharomyces cerevisiae*. J. Cell Biol. **122:** 635–644.

ITO, H., Y. FUKUTA and A. KIMURA, 1983 Transformation of intact yeast cells treated with alkali cations. J. Bacteriol. **150:** 163–168.

JANSEN, R-P., C. DOWZER, C. MICHAELIS, M. GALOVA and K. NASMYTH, 1996 Mother cell-specific *HO* expression in budding yeast depends on the unconventional myosin Myo4p and other cytoplasmic proteins. Cell **84:** 687–697.

JOHNSON, D. I., and J. R. PRINGLE, 1990 Molecular characterization of *CDC42*, a *Saccharomyces cerevisiae* gene involved in the development of cell polarity. J. Cell Biol. **111:** 539–551.

JOHNSTON, G. C., J. A. PRENDERGAST and R. A. SINGER, 1991 The *Saccharomyces cerevisiae MYO2* gene encodes an essential myosin for vectorial transport of vesicles. J. Cell Biol. **113:** 539–551.

KAISER, C. A., and R. SCHEKMAN, 1990 Distinct sets of *SEC* genes govern transport vesicle formation and fusion early in the secretory pathway. Cell **61:** 723–733.

KARPOVA, T. S., M. MARC and J. A. COOPER, 1993 Mutations that enhance the *cap2* null mutant phenotype in *Sacchromyces cerevisiae* affect the actin cytoskeleton, morphogenesis and pattern of growth. Genetics **135:** 693–709.

KILMARTIN, J., and A. E. M. ADAMS, 1984 Structural rearrangements of tubulin and actin during the cell cycle of the yeast *Saccharomyces*. J. Cell Biol. **98:** 922–933.

KIM, Y. J., L. FRANCISCO, G. C. CHEN, E. MARCOTTE and C. S. M. CHAN, 1994 Control of cellular morphogenesis by the *Ipt2/Bem2* GTPase-activating protein: possible role of protein phosphorylation. J. Cell Biol. **127:** 1381–1394.

KUBLER, E., and H. RIEZMAN, 1993 Actin and fimbrin are required for the internalization step of endocytosis in yeast. EMBO J. **12:** 2855–2862.

LEW, D. J., and S. I. REED, 1993 Morphogenesis in the yeast cell cycle: regulation by *CDC28* and cyclins. J. Cell Biol. **120:** 1305–1320.

LEW, D. J., and S. I. REED, 1995 A cell cycle checkpoint monitors cell morphogenesis in budding yeast. J. Cell Biol. **129:** 739–749.

LIU, H., and A. BRETSCHER, 1989a Disruption of the single tropomyosin gene in yeast results in the disappearance of actin cables from the cytoskeleton. Cell **57:** 233–242.

LIU, H., and A. BRETSCHER, 1989b Purification of tropomyosin from *Saccharomyces cerevisiae* and identification of related proteins in *Schizosaccharomyces* and *Physarum*. Proc. Natl. Acad. Sci. USA **86:** 90–93.

LIU, H., and A. BRETSCHER, 1992 Characterization of *TPM1* disrupted yeast cells indicates an involvement of tropomyosin in directed vesicular transport. J. Cell Biol. **118:** 285–299.

MADAULE, P., R. AXEL and A. M. MYERS, 1987 Characterization of two members of the rho gene family from the yeast *Sacchromyces cerevisiae*. Proc. Natl. Acad. Sci. USA **84:** 779–783.

MADAULE, P., J. S. JOHNSON, M. MCCAFFRAY, P. BOQUET and A. M. MYERS, 1994 Rho1p of *S. cerevisiae*, in *Guidebook to the Small GTPases*, edited by L. A. HUBER, M. ZERIAL and J. TOOZE. Oxford University Press, Oxford.

MATSUI, Y., and A. TOH-E, 1992a Yeast *RHO3* and *RHO4* ras superfamily genes are necessary for bud growth, and their defect is suppressed by a high dose of bud formation genes *CDC42* and *BEM1*. Mol. Cell. Biol. **12:** 5690–5699.

MATSUI, Y., and A. TOH-E, 1992b Isolation and characterization of two novel ras superfamily genes in *Saccharomyces cerevisiae*. Gene **114:** 43–49.

MAZZONI, C., P. ZARZOV, A. RAMBOURG and MANN, C, 1993 The *SLT2* (*MPK1*) MAP kinase homolog is involved in polarized cell growth in *Sacchromyces cerevisiae*. J. Cell Biol. **123:** 1821–1833.

MICHAELIS, S, 1994 A non-specific mechanism for protein secretion: export of yeast a-factor by the ABC transporter, *STE6*. Mol. Biol. Cell. Suppl. **5:** 251A.

NONAKA, H., K. TANAKA, H. HIRANO, T. FUJIWARA, H. KOHNO *et al.*, 1995 A down stream target of *RHO1* small GTP-binding protein is *PKC1*, a homolog of protein kinase C, in *Sacchromyces cerevisiae*. EMBO J. **14:** 5931–5938.

PALMER R. E., D. S. SULLIVAN, T. HUFFAKER and D. KOSHLAND, 1992 Role of astral microtubules and actin in spindle orientation and migration in budding yeast, *Sacchromyces cerevisiae*. J. Cell Biol. **119:** 583–593.

PRINGLE, J. R., R. A. PRESTON, A. E. M. ADAMS, T. STERNS, D. G.

DRUBIN *et al.*, 1989 Fluorescence microscopy methods for yeast. Methods Cell Biol. **81:** 357–435.

QADOTA, H., C. P. PYTHON, S. B. INOUE, M. ARISAWA, Y. ANRAKU *et al.*, 1996 Identification of yeast Rho1p GTPase as a regulatory subunit of 1,3-β-glucan synthase. Science **272:** 279–281.

RIEZMAN, H, 1985 Endocytosis in yeast: several of the yeast secretory mutants are defective in endocytosis. Cell **40:** 1001–1009.

ROEMER, T., L. G. VALLIER and M. SNYDER, 1996 Selection of polarized growth sites in yeast. TICB **6:** 434–441.

SALMINEN, and P. NOVICK, 1987 ras-like protein is required for a post-Golgi event in yeast secretion. Cell **49:** 527–538.

SHERMAN, F., 1991 Getting started with yeast. Methods Enzymol. **194:** 3–21.

SHORTLE, D., J. E. HABER and D. BOTSTEIN, 1982 Lethal disruption of the yeast actin gene by integrative DNA transformation. Science **217:** 371–373.

SIKOSKI, R. S., and P. HIETER, 1989 A system of shuttle vectors and yeast host strains designed for efficient manipulation of DNA in *Saccharomyces cerevisiae.* Genetics **122:** 19–27.

SIMON, V. R., T. C. SWAYNE and L. A. PON, 1995 Actin-dependent mitochondrial motility in mitotic yeast and cell-free systems: identification of a motor activity on the mitochondrial surface. J. Cell Biol. **130:** 345–354.

SPRAGUE, G. F., JR., 1991 Assay of yeast mating reaction. Methods Enzymol. **194:** 77–94.

VIDA, T. A., and S. D. EMR, 1995 A new vital stain for visualizing vacuolar membrane dynamics and endocytosis in yeast. J. Cell Biol. **128:** 779–792.

WANG, T., and A. BRETSCHER, 1995 The rho-GAP encoded by *BEM2* regulates cytoskeletal structure in budding yeast. Mol. Biol. Cell **6:** 1011–1024.

WELCH, M. D., D. A. HOLTZMAN and D. G. DRUBIN, 1993 The yeast cytoskeleton. Curr. Opin. Cell Biol. **6:** 110–119.

YAMOCHI, W., K. TANAKA, H. NONAKA, A. MAEDA, T. MUSHA *et al.*, 1994 Growth site localization of Rho1 small GTP-binding protein and its involvement in bud formation in *Saccharomyces cerevisiae.* J. Cell Biol. **125:** 1077–1093.

YANG, S., K. R. AYSCOUGH and D. G. DRUBIN, 1997 Role for the actin cytoskeleton of *Sacchromyces cerevisiae* in bipolar bud-site selection. J. Cell Biol. **136:** 111–123.

ZARZOV, P., C. MAZZONI and C. MANN, 1996 The *SLT2* (*MPK1*) MAP kinase is activated during periods of polarized cell growth in yeast. EMBO J. **15:** 83–91.

Communicating editor: M. D. ROSE